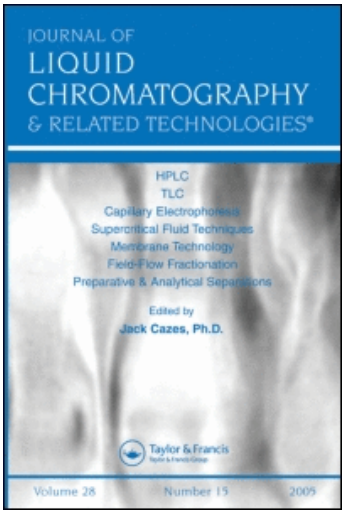

Journal of Liquid Chromatography & Related Technologies
Publication details, including instructions for authors and subscription information:
http://www.informaworld.com/smpp/title~content=t713597273

Simultaneous Optimization of Product Purity and Yield in a Simulated Moving Bed Chromatography for Nystatin Purification

Sungyong Mun[a]
[a] Department of Chemical Engineering, Hanyang University, Seoul, Korea

To cite this Article Mun, Sungyong(2009) 'Simultaneous Optimization of Product Purity and Yield in a Simulated Moving Bed Chromatography for Nystatin Purification', Journal of Liquid Chromatography & Related Technologies, 32: 1, 1 — 27
To link to this Article: DOI: 10.1080/10826070802548523
URL: http://dx.doi.org/10.1080/10826070802548523

Journal of Liquid Chromatography & Related Technologies®, 32: 1–27, 2009

ISSN: 1082-6076 print/1520-572X online
DOI: 10.1080/10826070802548523

Simultaneous Optimization of Product Purity and Yield in a Simulated Moving Bed Chromatography for Nystatin Purification

Sungyong Mun

Department of Chemical Engineering, Hanyang University, Seoul, Korea

Abstract: In this study, we accomplished the task of optimizing the product purity and yield simultaneously for a four zone simulated moving bed (SMB) chromatographyaiming at the purification of nystatin, which is one of the well known antifungal antibiotics. For this work, a multi-objective optimization principle was adopted while employing the purity and yield of product (nystatin) as the objective functions. The results from such a multi-objective optimization task were obtained in the form of a Pareto optimal set, which comprises a group of multiple solutions that have equal optimum status in terms of both the nystatin purity and yield. The optimal solutions in the Pareto set showed a trade-off between the two objectives, which could be well interpreted using the equilibrium theory. The effect of adsorbent particle size on the above optimization results was investigated. With the increase of the particle size, the nystatin purities and yields of the SMBs corresponding to the Pareto set were found to increase in the region of small particles (pressure limiting region) but decrease in the region of large particles (mass transfer limiting region). As a result, the best Pareto set, which is defined here as the Pareto set surpassing all the other ones in both the nystatin purity and yield, occurs when the particle size falls on the boundary between the pressure limiting and the mass transfer limiting regions. The effect of throughput (or feed flow rate) on the optimization results was also examined. The results showed that a decrease in the throughput improved the nystatin purity and yield while narrowing down the distribution region of the two objective values on the corresponding best Pareto curve. Consequently, the highest purity and yield of nystatin (99.9% each) were attained

Correspondence: Prof. Sungyong Mun, Department of Chemical Engineering, Hanyang University, Haengdand-dong, Seongdong-gu, Seoul 133-791, Korea
E-mail: munsy@hanyang.ac.kr

when the best Pareto curve was converged to only a single point as a result of a significant decrease in the throughput.

Keywords: Nystatin purification, Simultaneous optimization, SMB chromatography

INTRODUCTION

Nystatin is a major constituent of a relatively large group of highly unsaturated antifungal antibiotics.[1] It has been regarded as a relatively safe drug for treating oral or gastrointestinal fungal infections.[1] According to the literature,[1,2] nystatin is produced by fermentation involving various strains of streptomycete species of microorganisms. During the fermentation, an undesired by-product, which virtually corresponds to an impurity component, is also known to be generated.[1] The need for a purification task has thus been an important issue in the nystatin production. Such a purification task has been previously conducted with a liquid chromatograph,[1] in which a reversed phase C_{18} media and the aqueous solution of methanol were employed as stationary and mobile phases, respectively.

There have been two different types of chromatographic processes available in the operation of liquid chromatography for purification purpose. One of them is a conventional batch chromatographic process, which has only one inlet and one outlet port. But its application has been limited mostly to laboratory scale. For preparative or large scale production, simulated moving bed (SMB) chromatography, which allows continuous countercurrent separation, is preferred because it can exploit both the properties of recycle chromatography and a carousel process.[3,4]

Figure 1 shows a schematic diagram of a four zone SMB chromatographic process for binary separation. More than four identical columns, which are packed with the same adsorbent particles, are connected to create a closed loop (Figure 1). It has two inlet ports (feed and desorbent) and two outlet ports (extract and raffinate), which play a role in partitioning the closed loop into four zones. Under such an arrangement, a countercurrent flow between mobile and stationary phases is actualized by moving the ports by one column in the direction of the mobile phase flow at a predetermined time interval (or switching time). If the flow rates and port switching time are properly designed, most of low affinity solute molecules (or fast migrating solute molecules) can be recovered from the raffinate port, while most of high affinity solute molecules (or slow migrating solute molecules) can be recovered from the extract port. This

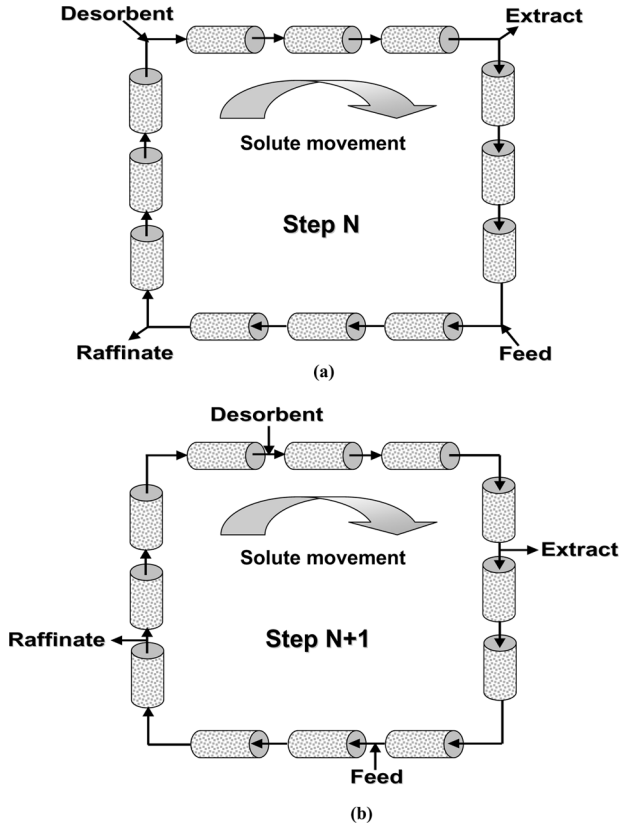

Figure 1. Schematic diagram of a four zone SMB chromatographic process for binary separation. (a) Step N, (b) Step N + 1.

is obviously favorable for attaining desired purity and yield of product. Furthermore, the aforementioned SMB operation principle allows a partial overlap between the two migrating solute bands without affecting adversely product purity and yield. For this reason, an SMB can achieve higher throughput, higher bed utilization, and lower desorbent consumption, than a batch chromatographic process.[3–6]

In the purification system of our interest, nystatin corresponds to a high affinity component and the related impurity a low-affinity one.[1] Thus, nystatin (product of interest) is collected from the extract port in a four zone SMB under consideration, and the impurity component is removed from the raffinate port. One of the important issues in designing such an SMB system is to improve the quality of nystatin product in the extract stream while reducing the amount of its loss through the raffinate port. The former is virtually to optimize the SMB for increasing the

nystatin purity, while the latter is to optimize the SMB for increasing the nystatin yield (or recovery). Either of the two optimizations tasks can be carried out individually using conventional single objective optimization techniques. However, it is often more important and more valuable to optimize the two objectives (product purity and yield) simultaneously, which will require a highly advanced optimization algorithm other than conventional single objective optimization techniques.[7–10]

The goal of this study is to accomplish the aforementioned simultaneous optimization of product purity and yield for four zone SMB chromatography aiming at nystatin purification on the basis of a multi-objective optimization principle. Effects f adsorbent particle size or throughput on such a multi-objective optimization result will also be investigated. Furthermore, this study will examine which factor actually restricts the nystatin purity and yield of an optimized SMB system.

The multi-objective optimization technique, which is used as a major tool of optimization in the present study, has been established previously through a series of intensive researches.[7–10] Many publications reported its successful applications to many of engineering problems.[9] One of the major features of a multi-objective optimization task is that it produces multiple optimum solutions instead of a single optimum solution. These types of multiple solutions is known as Pareto optimal solutions or Pareto set,[7] where every solution has equal optimum status in terms of all the objective functions considered. Thus, the selection of only one desired solution from a set of the Pareto optimal solutions is entirely dependent on other economic factors or market circumstances.

For the multi-objective optimization of our interest, the model equations regarding a four zone SMB system for nystatin purification are needed. In this study, the standing wave design (SWD) equations[11] are chosen to describe the SMB of interest, because the SWD has been one of the well known models for the optimal design of SMB. Furthermore, the SWD has been validated both theoretically and experimentally in many previous researches.[11,12]

THEORY

In the multi-objective optimization tool employed, the mathematics portion for the SMB system is handled by the SWD as stated above. For better understanding of the SWD, its fundamental principle is explained in this section. Since its concept originates from a wave dynamics peculiar to SMB, we will first give a brief explanation on the difference between batch and SMB wave formations. Then, a detailed statement on the SWD equations and principle will be made, including its mathematical merits.

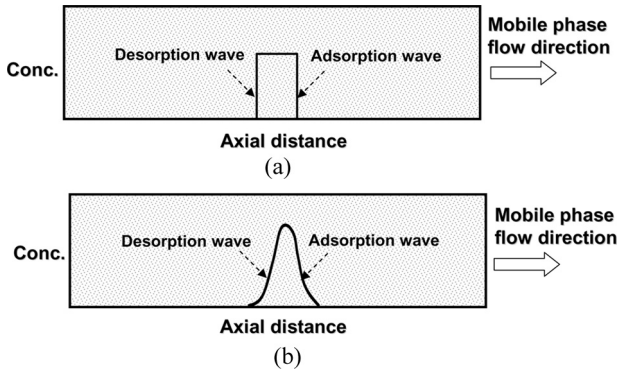

Figure 2. Concentration waves of a solute band migrating through a chromatographic bed. (a) Ideal, (b) Non-ideal.

Concentration Waves in Batch and SMB Chromatographic Processes

If a certain amount of feed solution is injected into a chromatographic bed, it forms a solute band, which migrates along the bed. Such a migrating solute band is usually marked by two concentration waves as shown in Figure 2. One is the adsorption wave (front boundary of a solute band) and the other the desorption wave (rear boundary of a solute band). Such concentration waves become square waves with infinitely sharp boundaries in the case of an ideal system where no mass transfer effects are present (Figure 2a). By contrast, in a non ideal system where mass transfer effects are not negligible, the concentration waves become spread as shown in Figure 2b.

If a feed solution contains a binary mixture, two different solute bands are formed inside the chromatographic bed. Since each solute band is accompanied by two concentration waves (adsorption and desorption waves), a binary system results in a total of four concentration waves.

To purify the solute of interest from a binary mixture in conventional batch chromatography, the two solute bands should be eluted along the bed until their overlap almost disappears, i.e., the adsorption wave of a slow migrating solute and the desorption wave of a fast migrating solute are almost separated. This principle, however, requires a large amount of desorbent and brings about a significantly low utilization of the adsorbent bed, which places a limitation on obtainable throughput and yield.

These operational disadvantages can be overcome by using SMB chromatography, in which a successful purification task is practicable even in the presence of a significant overlap between the two solute bands.[3–5] This condition obviously leads to an increase in adsorbent

utilization and a reduction in desorbent consumption. To create such a favorable condition, the migration range of each concentration wave needs to be kept within a properly predetermined part of the SMB bed.

As shown in Figure 3, the desorption wave of a slow migrating solute is to be confined in zone I while its adsorption wave in zone III. Simultaneously, the desorption and adsorption waves of a fast migrating solute are to be confined in zones II and IV, respectively. Under this situation, a feed solution can always be loaded into the mixed region while a pure product and an impurity can always be drawn from the separated region, resulting in high purity and high yield (Figure 3).

Standing Wave Design (SWD)

To maintain the aforementioned wave conditions, a set of SMB operating parameters such as four zone flow rates and switching time should be determined properly. Such a task has been referred to as "SMB design" in the literature.[3,5,11] One of the trustworthy ways of designing an SMB optimally is to use the standing wave design (SWD) method, which has been developed previously.[11]

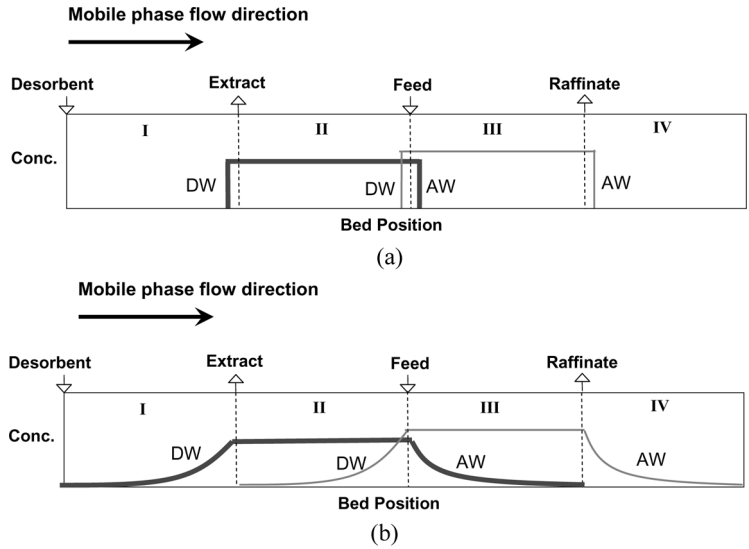

Figure 3. Concentration waves of a solute band in SMB system with linear isotherm. (a) Ideal, (b) Non-ideal. The thin and thick lines indicate the fast migrating (low affinity) and the slow migrating (high affinity) components, respectively. DW and AW stand for desorption and adsorption waves, respectively.

The basic principle of the SWD is to select the four zone flow rates and switching time such that each concentration wave can be made standing in its respective zone on the time-averaged sense.[11] The main idea of realizing such a principle is to match the migration velocity of a key concentration wave in each zone with the time averaged port velocity.[11] This concept can be represented mathematically as follows for an ideal system,

$$u_{w,i}^{j} = \nu\left(= \frac{L_c}{t_s}\right) \tag{1}$$

where $u_{w,i}^{j}$ is the wave migration velocity of a solute i in zone j, and ν is the port velocity (=single column length (L_c)/switching time (t_s)). According to the reference,[13] the wave velocity can be expressed in terms of volumetric flow rate and intrinsic parameters as follows:

$$u_{w,i}^{j} = \frac{Q^j}{S \cdot [\varepsilon_b + (1 - \varepsilon_b) \cdot \delta_i]} \tag{2}$$

where Q^j is the volumetric flow rate in zone j; S is the cross-sectional area of a column; ε_b is the inter-particle void fraction; and δ_i is defined as $\varepsilon_p + (1 - \varepsilon_p) \cdot a_i$, where ε_p is the intra-particle void fraction and a_i is the linear isotherm parameter. Combination of the above two equations (1) and (2) leads to a series of SWD equations for a linear, ideal system as follows:[11]

$$Q^I = S \cdot [\varepsilon_b + (1 - \varepsilon_b) \cdot \delta_A] \cdot L_c/t_s \tag{3a}$$

$$Q^{II} = S \cdot [\varepsilon_b + (1 - \varepsilon_b) \cdot \delta_B] \cdot L_c/t_s \tag{3b}$$

$$Q^{III} = S \cdot [\varepsilon_b + (1 - \varepsilon_b) \cdot \delta_A] \cdot L_c/t_s \tag{3c}$$

$$Q^{IV} = S \cdot [\varepsilon_b + (1 - \varepsilon_b) \cdot \delta_B] \cdot L_c]/t_s \tag{3d}$$

where the superscripts I to IV stand for zone number, and the subscripts A and B indicate the slow migrating (or high-affinity) and the fast migrating (or low affinity) solutes, respectively.

For a linear, non ideal system (with significant mass transfer effects), the above SWD equations, which were developed for an ideal system, need to be adjusted to counter wave spreading that occurs due to dispersion and mass transfer resistances. For such an adjustment, the SWD equations for a non ideal system includes additional correction terms, which are functions of mass transfer parameters, zone lengths, isotherm

parameters, and a decay factor as follows:[11]

$$Q^I = S \cdot [\varepsilon_b + (1-\varepsilon_b)\cdot\delta_A]\cdot L_c/t_s + \frac{\varepsilon_b \cdot S \cdot \beta_A^I}{N_c^I \cdot L_c}\left[E_{b,A}^I + \frac{P\cdot(\delta_A \cdot L_c/t_s)^2}{K_{f,A}^I}\right] \tag{4a}$$

$$Q^{II} = S \cdot [\varepsilon_b + (1-\varepsilon_b)\cdot\delta_B]\cdot L_c/t_s + \frac{\varepsilon_b \cdot S \cdot \beta_B^{II}}{N_c^{II} \cdot L_c}\left[E_{b,B}^{II} + \frac{P\cdot(\delta_B \cdot L_c/t_s)^2}{K_{f,B}^{II}}\right] \tag{4b}$$

$$Q^{III} = S \cdot [\varepsilon_b + (1-\varepsilon_b)\cdot\delta_A]\cdot L_c/t_s - \frac{\varepsilon_b \cdot S \cdot \beta_A^{III}}{N_c^{III} \cdot L_c}\left[E_{b,A}^{III} + \frac{P\cdot(\delta_A \cdot L_c/t_s)^2}{K_{f,A}^{III}}\right] \tag{4c}$$

$$Q^{IV} = S \cdot [\varepsilon_b + (1-\varepsilon_b)\cdot\delta_B]\cdot L_c/t_s - \frac{\varepsilon_b \cdot S \cdot \beta_B^{IV}}{N_c^{IV} \cdot L_c}\left[E_{b,B}^{IV} + \frac{P\cdot(\delta_B \cdot L_c/t_s)^2}{K_{f,B}^{IV}}\right] \tag{4d}$$

where N_c^j is the number of columns in zone j; P is the phase ratio, defined as $(1\text{-}\varepsilon_b)/\varepsilon_b$; E_b is the axial dispersion coefficient; and β is a decay factor that is related to yield and zone linear velocity. If the yield of each component is given, the β values are determined from component mass balance equations.[14] The lumped mass transfer coefficient (K_f) can be estimated from the following equation:[11]

$$\frac{1}{K_f} = \frac{R^2}{15\varepsilon_p D_p} + \frac{R}{3k_f} \tag{5}$$

where R is the radius of adsorbent particle; D_p is the effective pore diffusivity; and k_f is the film mass transfer coefficient.

To exploit the above SWD equations for SMB optimization, a series of intrinsic parameters, including void fraction, dispersion, and mass transfer coefficients, and linear isotherms, are required. All of these intrinsic parameters for the nystatin purification system were reported by Jensen et al.[1] and they are listed in Table 1.

It is emphasized here that the SWD equations do not include any ordinary or partial differential equations but consist of only algebraic equations. Thus, no iteration or trial and error is required in the calculation of the SWD.[13] Such a computational efficiency of the SWD is certainly advantageous to a multi-objective optimization task because it involves a huge number of SWD calculations.

Table 1. Intrinsic parameters of the nystatin purification system

	Nystatin	Impurity
Isotherm parameter (L/L S.V.)	2.06	1.05
Molecular diffusivity (cm^2/min)	6.0×10^{-4}	6.0×10^{-4}
Effective pore diffusivity (cm^2/min)	4.5×10^{-5}	4.5×10^{-5}
Film mass-transfer coefficient (cm/min)	The Wilson and Geankoplis correlation[22]	
Axial dispersion coefficient (cm^2/min)	The Chung and Wen correlation[23]	
Inter-particle void fraction	0.65	
Intra-particle void fraction	0.30	

Limiting Factor in SMB Separation Performance

The separation performance of SMB, which is usually evaluated by productivity, yield, or purity, is limited by one of the following two factors: (1) pressure drop constraint and (2) mass transfer efficiency (or column efficiency). Between the two limiting factors, the former is taken into account because the mechanical strength of adsorbent particles and other hardware conditions have finite limitations. The latter factor controls the degree of a solute wave spreading due to dispersion and mass transfer resistances, which has a critical effect on the separation efficiency.

In this study, the pressure drop of a four zone SMB unit was taken as the sum of the pressure drops occurring in each of the four zones, which was estimated using the Ergun equation.[15]

$$\Delta P = \sum_{j=I}^{IV} \Delta P^j = \sum_{j=I}^{IV} N_c^j \left(\frac{150\mu_0^j \cdot L_c}{d_p^2} \left(\frac{1-\varepsilon_b}{\varepsilon_b} \right)^2 \frac{10^6}{6} + \frac{1.75\rho(u_0^j)^2 L_c}{d_p} \left(\frac{1-\varepsilon_b}{\varepsilon_b} \right) \frac{1}{3.6} \right) \frac{14.7}{1.013 \times 10^5} \tag{6}$$

where ΔP is the total pressure drop through an SMB unit; d_p is the diameter of adsorbent particle, ρ and μ are the density and viscosity of mobile phase, respectively; and u_0^j is the interstitial linear velocity in zone j.

The mass transfer efficiency can be assessed by the dimensionless number, NTP (number of theoretical plates)[13] or DI (deviation from ideality).[16] In this study, the latter was adopted to quantify the degree of mass transfer efficiency because its theoretical background came from

the SWD equations. The dimensionless number DI for component i in zone j is given by:[16]

$$DI_i^j \equiv \frac{1}{Pe_i^j} + \frac{1}{St_i^j}\left(\frac{1-\varepsilon_b}{\varepsilon_b}\right)(\delta_i)^2\left(\frac{L_c/t_s}{u_0^j}\right)^2\left(\frac{R}{N_c^j L_c}\right) \tag{7}$$

where the Peclet number (Pe_i^j) and the Stanton number (St_i^j) are defined as:

$$Pe_i^j = \frac{u_0^j \cdot N_c^j \cdot L_c}{E_i^j} \tag{8a}$$

$$St_i^j = \frac{K_{f,i}^j R}{u_0^j} \tag{8b}$$

As the DI value is larger, solute waves are subject to more significant dispersion and mass transfer resistances. Therefore, the solute waves under a larger DI become more spread, resulting in a lower mass transfer efficiency (or column efficiency).

FORMULATION OF OPIMIZATION PROBLEM

The optimization problem considered is the simultaneous maximization of product (nystatin) purity and yield under a given throughput (or feed flow rate) in a four zone SMB for nystatin purification. As a model equation for such an SMB optimization, the above explained SWD was adopted in the present study. During the optimization, the following two constraints were taken into account. First, the purity and yield of nystatin should be higher than 85%. Secondly, the total pressure drop through the SMB unit must not exceed 100 psi, which is a general criterion for a low pressure SMB process. Such an optimization problem can be represented mathematically as follows:

$$\text{Max} \quad J_1 = \text{Pur}_A\,[Q^I,\ Q^{II},\ Q^{III},\ Q^{IV},\ t_s,\ \text{Yield}_A,\ \text{Yield}_B,\ \chi] \tag{9a}$$

$$\text{Max} \quad J_2 = \text{Yield}_A\,[Q^I,\ Q^{II},\ Q^{III},\ Q^{IV},\ t_s,\ \text{Yield}_A,\ \text{Yield}_B,\ \chi] \tag{9b}$$

$$\text{Subject to} \quad \text{Pur}_A \geq 85.0\%,\ \text{Yield}_A \geq 85.0\%, \tag{9c}$$

$$\Delta P \leq 100 \text{ psi} \tag{9d}$$

$$Q^{III} - Q^{II} = Q_{Feed}(\text{targeted feed flow rate}) \tag{9e}$$

$$2 \leq N_c^j \leq 4 \tag{9f}$$

$$\text{Fixed variables } C_F = 1.0\,\text{g/L for each component} \tag{9g}$$

$$L_c = 30\,\text{cm},\ d_c = 4\,\text{cm}, N_{c,\text{total}} = 12 \tag{9h}$$

where Pur_A and $Yield_A$ are the purity and yield of a product component (nystatin), respectively; $Yield_B$ is the yield of an impurity component; χ stands for column configuration; and $N_{c,\text{total}}$ is the total number of columns used in SMB unit.

Note in the above equations (9a) and (9b) that the yields of both components were included as the variables to be optimized (or decision variables). This is because the yield values are used to specify the decay factors (β) in the SWD equations, i.e., serve as input data for the SWD.

As indicated by Equation (9h), the dimension of each column and the total column number are kept fixed during the optimization. This means that the total bed volume remains constant. In this case, throughput is virtually determined by feed flow rate alone and thus, the two values can be used interchangeably. Since throughput is treated as a target value in this study, feed flow rate is also kept constant in each optimization task. In order to investigate the effect of changing throughput on the optimization results, the aforementioned optimization task will be performed under three different throughputs (the feed flow rates of 60, 80, and 100 mL/min).

Besides the throughput, the adsorbent particle size also has a significant effect on the product purity and yield via pressure drop and mass transfer efficiency, as expected from Equations (6) to (8). To reduce the computation time, the adsorbent particle size was not directly included as the decision variables, as can be seen in Equations (9a) and (9b). Instead, the adsorbent particle size was changed in a discrete manner and for each step the product purity and yield were optimized, followed by analyzing the effect of particle size on the optimization results.

To handle the aforementioned multi-objective optimization problem, a highly efficient adaptation of genetic algorithm, NSGA-II-JG,[8–10,17,18] was employed in this study. The principle of the NSGA-II-JG algorithm has been stated in detail elsewhere,[9,17,18] and its applications to SMB optimizations have been reported in several previous publications.[8,10,18]

RESULTS AND DISCUSSION

Simultaneous Optimization of Nystatin Purity and Yield

The purity and yield of nystatin were optimized simultaneously under the above stated constraints while keeping the target feed flow rate and the particle size fixed at 80 mL/min and 50 μm, respectively. The resulting Pareto optimal solutions are presented in Figure 4, in which a tradeoff

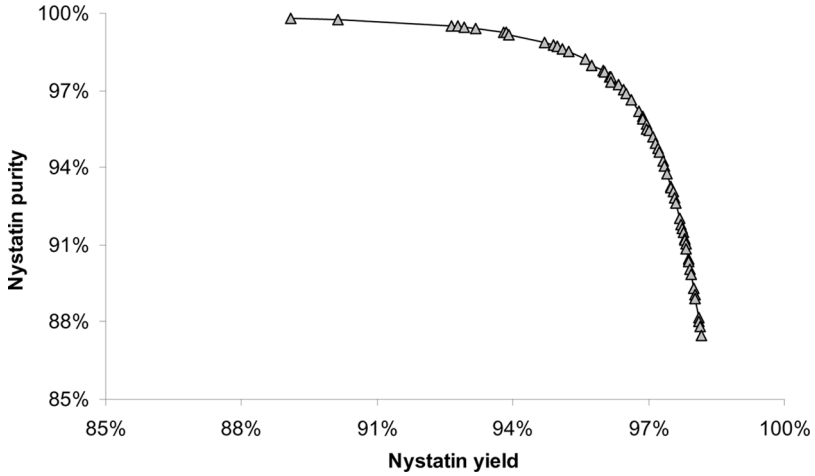

Figure 4. Pareto optimal solutions from the simultaneous optimization of the nystatin purity and yield under the particle size of 50 μm and the feed flow rate of 80 mL/min.

between the two objectives is demonstrated clearly. It can be easily confirmed that as the nystatin yield increases, its purity has a decreasing trend and vice versa. This phenomenon is typical of multi-objective optimization solutions, in which one objective function improves while one other deteriorates along the set of optimal solutions (or Pareto solutions). Therefore, any point along the Pareto curve has an equal optimum status from the standpoint of both the nystatin purity and yield.

To interpret the aforementioned trend more systematically, we use the frame of equilibrium theory,[19] which can provide a comprehensive picture of all possible performances of a continuous countercurrent chromatographic process via the following flow rate ratio, m^j, in each zone of an SMB.[19]

$$m^j = \frac{Q^j \cdot t_s - L_c \cdot S \cdot (\varepsilon_b + (1 - \varepsilon_b) \cdot \varepsilon_p)}{L_c \cdot S \cdot (1 - \varepsilon_b) \cdot (1 - \varepsilon_p)} \tag{10}$$

The above m^j value indicates the ratio of liquid (or mobile phase) flow rate in zone j to solid flow rate associated with periodic port movement. Thus, a larger m^j value results in a higher velocity of solute migration (in the direction of mobile phase flow) relative to the ports.

To analyze the optimization results in this section using the aforementioned frame, the m^j values for zone II and III, which correspond to the key separation zones in a four zone SMB, were calculated for each

solution point on the Pareto curve (Figure 4). The resulting m^{II} and m^{III} values are plotted in Figure 5a with respect to nystatin purity and in Figure 5b with respect to nystatin yield. Note that the m^{II} and m^{III} values are both on the increase or both on the decrease. Under such a situation, the nystatin purity shows an increasing trend as the m^{II} and m^{III} values increase at the same time (Figure 5a). In contrast, the nystatin yield becomes higher when the m^{II} and m^{III} values decrease at the same time (Figure 5b).

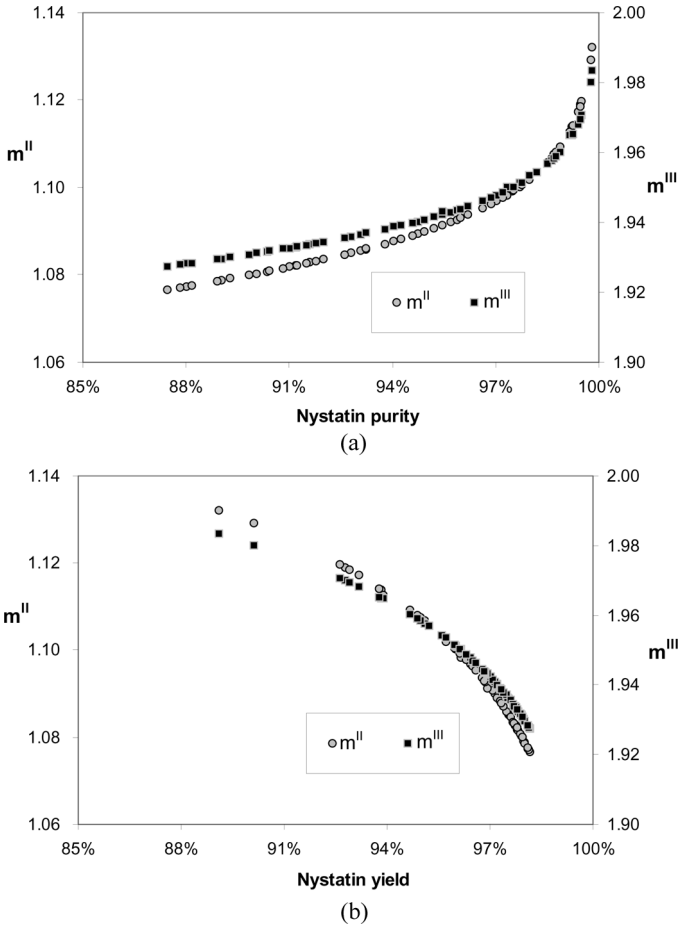

Figure 5. Plot of m^{II} and m^{III} values with respect to the nystatin purity or yield on the bases of the Pareto optimal solutions in Figure 4. (a) Nystatin purity versus m^{II} and m^{III}, (b) Nystatin yield versus m^{II} and m^{III}.

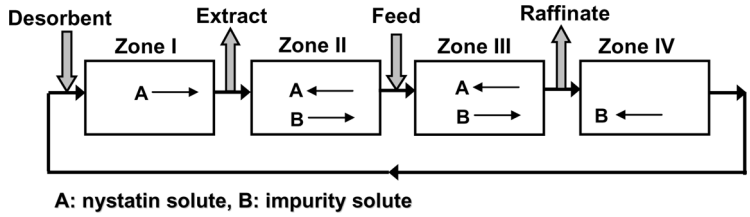

Figure 6. Desired pattern of solute migration relative to the ports for the attainment of complete separation in a four-zone SMB for nystatin purification.

The reason for such phenomena can be understood from Figure 6, where the desired pattern of solute migration (relative to the ports) for complete separation is illustrated in each zone by arrows. It is obvious that for higher nystatin purity, the impurity solute should be farther away from the extract port, i.e., the product port. To facilitate such behavior of impurity solute, its migration velocity relative to the ports in zones II and III should be higher, causing an increase in both the m^{II} and m^{III} values. This condition, however, promotes an increase in the migration velocity of nystatin in zones II and III, resulting in a loss of nystatin through the raffinate port and a reduction in the nystatin yield.

By contrast, a lower velocity of solute migration relative to the ports in zones II and III, which occurs as a result of a decrease in the m^{II} and m^{III} values, can improve the nystatin yield. This is because such a migration pattern prevents the nystatin solute from being lost through the raffinate port. However, the decrease in the m^{II} and m^{III} values makes the impurity solute closer to the extract port, thereby contaminating the nystatin product and reducing the nystatin purity.

Due to the aforementioned two phenomena, a tradeoff between the nystatin purity and yield is inevitable at the stage of the SMB optimization. The choice of only one optimal point from the Pareto set depends entirely on other economic factors such as feed price, solvent cost, adsorbent price, or product specification.

Effect of Adsorbent Particle Size on the Optimization Results

In this section, the above optimization task was repeated many times while varying the particle size in order to investigate its effect on the simultaneous optimization of the nystatin purity and yield.

The resulting Pareto sets based on different particle sizes are presented in Figures 7a and 7b. One of the noteworthy phenomena is that only a certain region of particle sizes (48 μm ~ 94 μum) can meet the constraints on the nystatin purity (≥85%) and yield (≥85%). If the particle

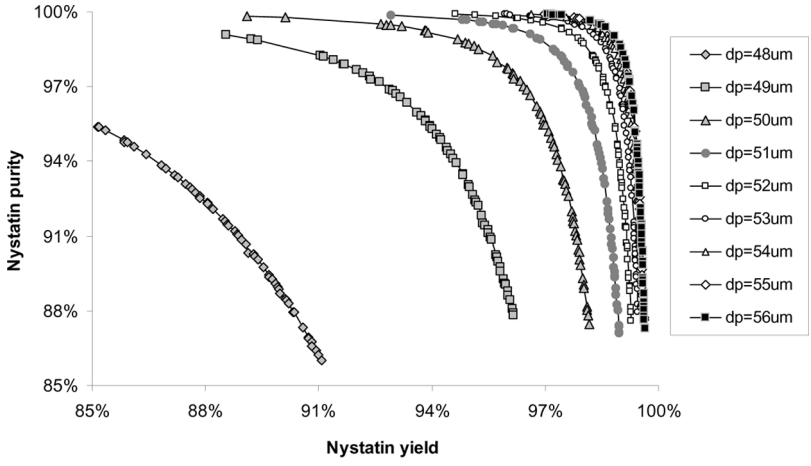

(a)

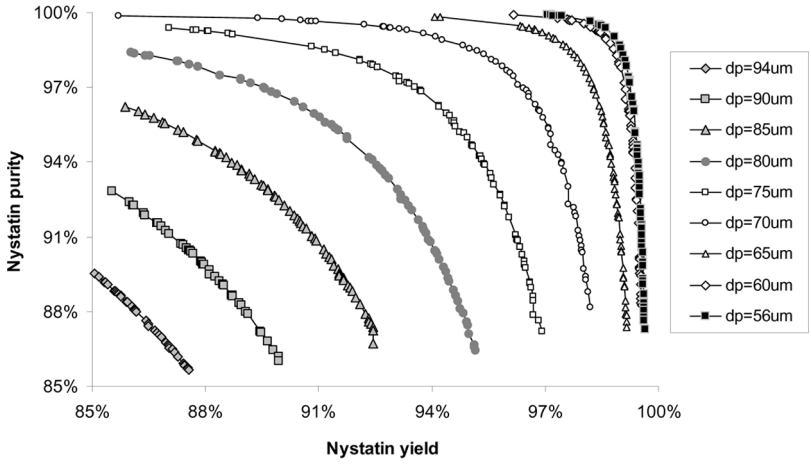

(b)

Figure 7. Effect of adsorbent particle size (d_p) on the Pareto set from the simultaneous optimization of the nystatin purity and yield under the feed flow rate of 80 mL/min. (a) Region of small particles (48 μm ~ 56 μum), (b) Region of large particles (56 μm ~ 94 μum).

size is below 48 μm or above 94 μum, the Pareto solutions are no longer generated from the optimization, which means that the resulting purity and/or yield of nystatin are less than 85%.

Another interesting observation is that in the region of small particles (<56 μm), the nystatin purity and yield become higher as the particle size

increases (Figure 7a). By contrast, in the region of large particles (>56 μm), the nystatin purity and yield decreases with increasing the particle size (Figure 7b). As a result, the best Pareto set, which is defined here as the Pareto set surpassing all the other Pareto sets in both the nystatin purity and yield, occurs at 56 μm.

To investigate the reason for the aforementioned phenomenon, the pressure drop of the SMB system was calculated for each point of the Pareto set using the Ergun equation (Equation (6)). Such calculations were performed for all the Pareto sets considered while varying the particle size. Note in Figure 8 that the resulting pressure drops are maintained at its upper limit (100 psi) while the particle size is kept below 56 μm. This result indicates that the two objective functions (i.e., nystatin purity and yield) of the SMB process with small particles (<56 μm) are virtually limited by the pressure drop. In such a pressure limiting region, the SMB process is operated at its maximum allowable flow rate, whose value varies according to the size of particle. According to the Ergun equation, the maximum allowable flow rate increases as the size of particle is larger under a fixed pressure drop. If the maximum allowable flow rate in SMB increases, it allows higher operational flexibility in making each key concentration wave standing in its respective zone, leading to better separation performance. Therefore, the nystatin purity and yield, if limited by the pressure drop, has an increasing trend as the particle size increases (Figure 7a).

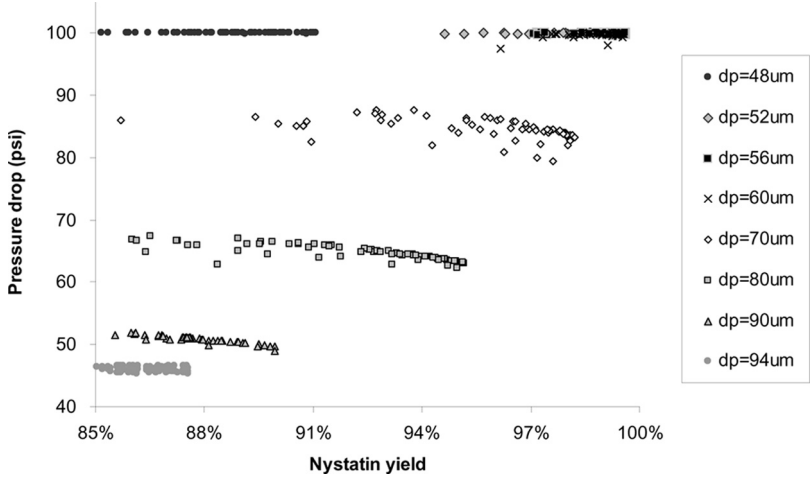

Figure 8. Effect of adsorbent particle size (d_p) on the pressure drops of the SMBs corresponding to the Pareto set from the simultaneous optimization of the nystatin purity and yield under the fixed feed flow rate of 80 mL/min.

By contrast, if the particle size is larger than 56 μm, the pressure drops of the corresponding SMBs along the Pareto curve are reduced to below 100 psi as shown in Figure 8. Under such circumstances, the nystatin purity and yield must be limited by other factors than the pressure drop. The factor limiting the nystatin purity and yield for large particles (>56 μm) is the mass transfer efficiency (or column efficiency), which can be evaluated by DI value based on the SWD equations.

Such DI values for the Pareto sets are presented in Figure 9 by varying the particle size. One can see that the DI value becomes higher as the particle size increases, which trend can be expected from Equation (7). As stated in the theory section, higher DI values indicates the occurrence of a larger dispersion and mass transfer resistances, thereby causing more significant spreading of solute bands in the SMB. This can obviously reduce the column efficiency, which in turn decreases the SMB separation performance. This is why the nystatin purity and yield decreases with increasing particle size in the region of large particles (>56 μm) (Figure 7b).

Considering all the issues discussed above, one can conclude that the optimal particle size for the best Pareto set in terms of both the nystatin purity and yield falls on the boundary between the pressure limiting and the mass transfer limiting regions.

Effect of Throughput (or Feed Flow Rate) on the Optimization Results

The feed flow rate in the previous optimizations was fixed at a target value (80 mL/min). The feed flow rate, however, sometimes needs to be changed, in case a raw material supply or a market demand varies to a considerable extent. Such a change in the feed flow rate will obviously have a significant effect on the nystatin purity and yield. To check this issue, another two optimizations were carried out for two other different feed flow rates, one of which was based on the lower feed flow rate (60 mL/min) and the other on the higher one (100 mL/min). The resulting Pareto sets for such two additional cases are presented in Figures 10 and 11. One can see that the best Pareto set, which is located farthest from both the x- and y- axes, occurs at the particle sizes of $45 \sim 55$ μm for the feed flow rate of 60 mL/min (Figure 10), and at the particle size of 63 μm for the feed flow rate of 100 mL/min (Figure 11). Recall that the best Pareto set for the feed flow rate of 80 mL/min occurs at the particle size of 56 μm (Figure 7).

Comparison of such best Pareto sets, based on different feed flow rates, reveals that as the feed flow rate decreases, the distribution region of the two objective values on the corresponding best Pareto curve is reduced. Eventually, when the feed flow rate is set at the lowest one

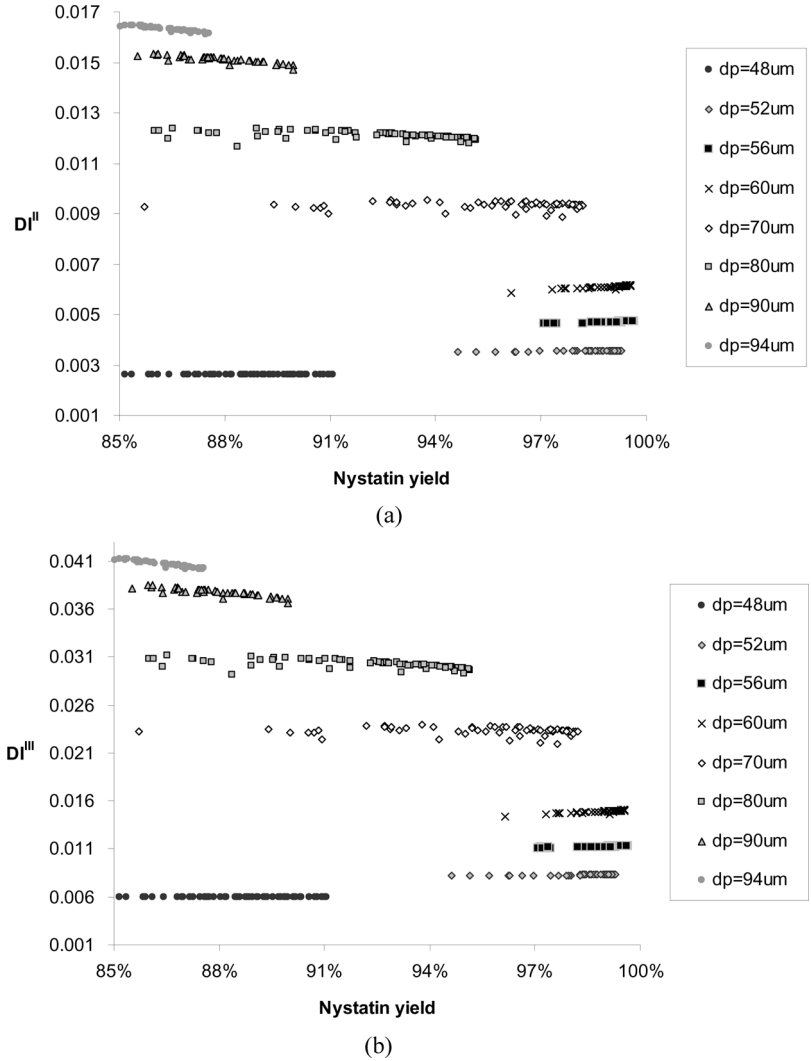

Figure 9. Effect of adsorbent particle size (d_p) on the DI values for zones II and III (key separation zones) of the SMBs corresponding to the Pareto set from the simultaneous optimization of the nystatin purity and yield under the fixed feed flow rate of 80 mL/min. (a) DI values for zone II, (b) DI values for zone III.

(60 mL/min), the corresponding best Pareto curve is found to be converged to only one point. The resulting purity and yield of nystatin at such a single Pareto point are found to be 99.9% each, which corresponds to the highest one attainable in this study.

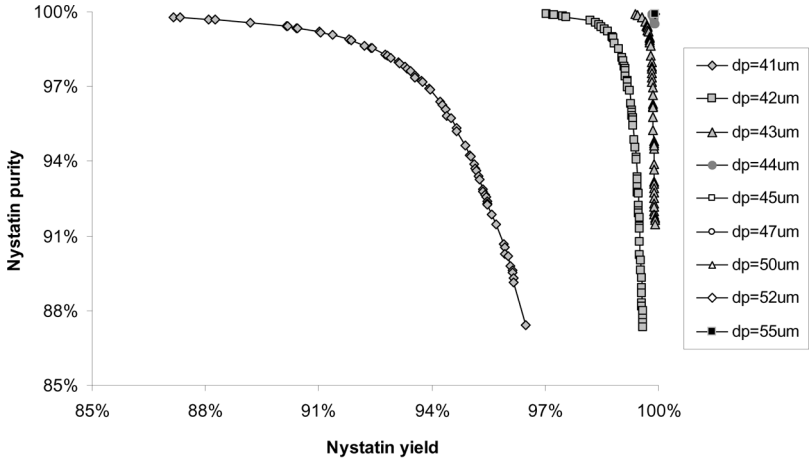

(a)

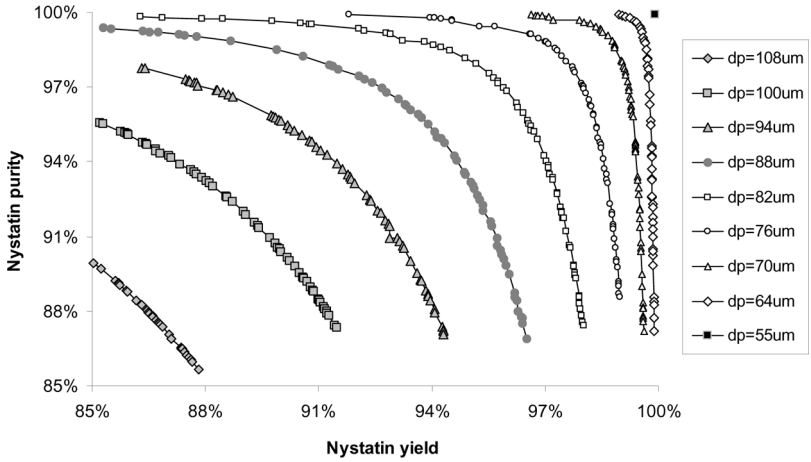

(b)

Figure 10. Pareto optimal solutions from the simultaneous optimization of the nystatin purity and yield under the feed flow rate of 60 mL/min. (a) Region of small particles (41 μm ~ 55 μm), (b) Region of large particles (55 μm ~ 108 μm).

Another noteworthy observation is that the effective range of particle size, which is defined here as the particle size range that can satisfy the constraints on the nystatin purity (≥85%) and yield (≥85%), becomes larger as the feed flow rate decreases. As can be seen in Table 2, the effective range of particle size can be enlarged by about 2.4 times if the feed flow rate is reduced from 100 to 60 mL/min. This result indicates that the

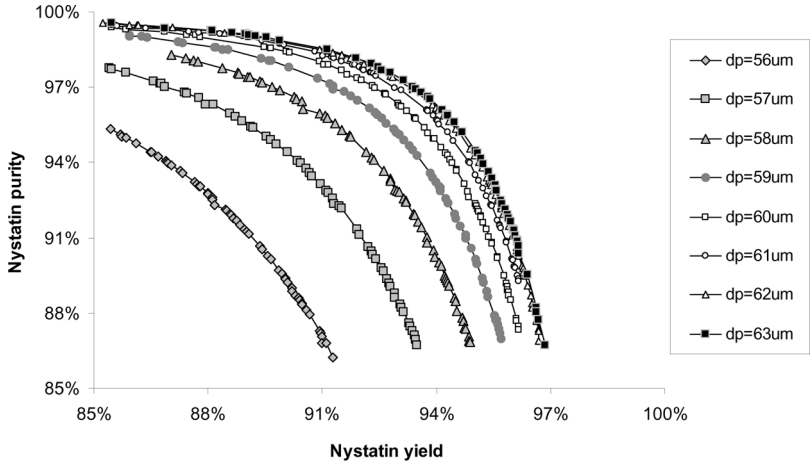

(a)

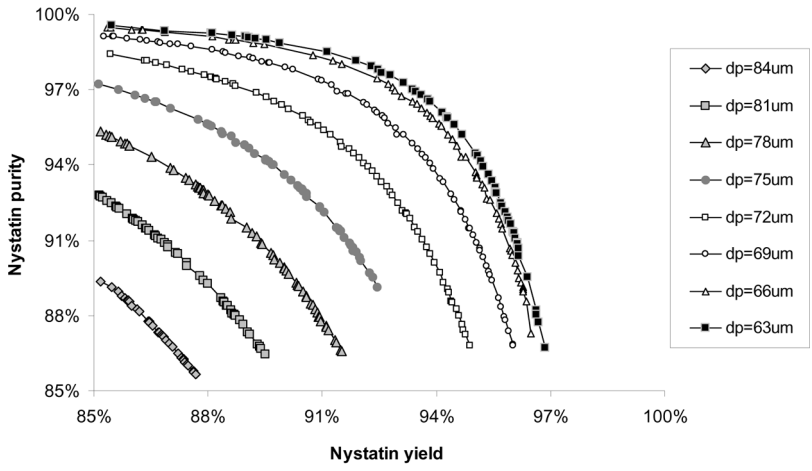

(b)

Figure 11. Pareto optimal solutions from the simultaneous optimization of the nystatin purity and yield under the feed flow rate of 100 mL/min. (a) Region of small particles (56 μm ~ 63 μm), (b) Region of large particles (63 μm ~ 84 μm).

SMB system based on a lower feed flow rate has more robustness with respect to a variation in the particle size.

Table 2 also lists the optimal particle size leading to the best Pareto set for each feed flow rate. Such an optimal particle size is found to be smaller as the feed flow rate decreases (Table 2). This is mostly because a decrease in the feed flow rate reduces the pressure drop of the SMB

Table 2. Influence of feed flow rate on the effective particle size range and the optimal particle size leading to the best Pareto set

Feed flow rate (mL/min)	Effective range of particle size (μm)	Optimal particle size leading to the best Pareto set (μm)
60	41∼108	45∼55
80	48∼94	56
100	56∼84	63

system. In this case, the SMB system can have some room for the use of smaller particles while meeting the pressure drop constraint. If smaller particles are used, the mass transfer efficiency (or column efficiency) is enhanced, as expected from Equation (7). Higher purity and yield of nystatin are therefore attainable with smaller particles, as long as the pressure drop constraint can be satisfied by decreasing the feed flow rate.

Wave Dynamics of Nystatin and Impurity in the SMB with the Highest Product Purity and Yield

In the previous section, it was found that the SMB system corresponding to the single Pareto solution, which resulted from the optimization under the feed flow rate of 60 mL/min and the particle size of 55 μm, gave the highest purity and yield of nystatin (99.9% each). For such an optimal SMB, its wave dynamics of nystatin and impurity are examined in this section to verify that its separation performance is actually realized. For this purpose, the column profiles of nystatin and impurity were obtained from detailed rate model simulations, which were conducted with an Aspen Chromatography 2004 simulator. The numerical parameters used are listed in Table 3, while the operating parameters and the column configuration of the optimal SMB under examination in Table 4.

Table 3. Numerical parameters used in the detailed rate-model simulations for the SMB corresponding to the best Pareto solution under the feed flow rate of 60 mL/min

Discretization method	Biased Upwind Differencing Scheme
Number of nodes per column	40
Integration method	Gear
Step size	0.05

Table 4. Operating parameters and column configuration of the SMB corresponding to the best Pareto solution (dp = 55 μm) under the feed flow rate of 60 mL/min

Zone I flow rate (mL/min)	611.496
Zone II flow rate (mL/min)	449.370
Zone III flow rate (mL/min)	509.370
Zone IV flow rate (mL/min)	410.598
Switching time (min)	0.87515
Column configuration*	2-4-4-2

Column configuration refers to the number of columns in each zone; 2-4-4-2 means that there are two columns in zone 1, four in zone II, four in zone III, and two in zone IV.

The column profiles resulting from such simulations are presented in Figure 12 when a cyclic steady state is reached. Although at such a cyclic steady state the position of a solute band relative to the feed port still varies with time, its migration pattern is repeated uniformly in every switching time. For this reason, the column profiles were obtained at three different times (Figure 12) as follows: the beginning, the middle, and the end of a switching period at cyclic steady state. Such three column profiles are sufficient to show the representative behavior of solute band migration.

As mentioned in the theory section, the solute band migrating through a chromatographic bed is usually accompanied by two concentration waves such as adsorption and desorption waves. It is the migration ranges of such two waves at cyclic steady state that virtually determine product purity and yield.[20,21] Note in Figure 12, that the desorption wave of nystatin is well confined within zones I from the beginning to the end of a switching period at cyclic steady state, while its adsorption wave within zones III. Simultaneously, the desorption and adsorption waves of impurity are well confined within zones II and IV, respectively, during the entire switching period (Figure 12). Such wave conditions are the chief factors in maintaining high purity (99.9%) and high yield (99.9%) for the nystatin product.

CONCLUSION

For a four zone SMB aiming at nystatin purification, the product purity and yield were optimized simultaneously in accordance with the multi-objective optimization principle. The standing wave design (SWD) equations were employed to handle the mathematical description for the SMB of interest in the multi-objective optimization tool considered. During the optimization, the following two constraints were taken into account; (1) purity and yield of nystatin $\geq$85% and (2) total pressure drop

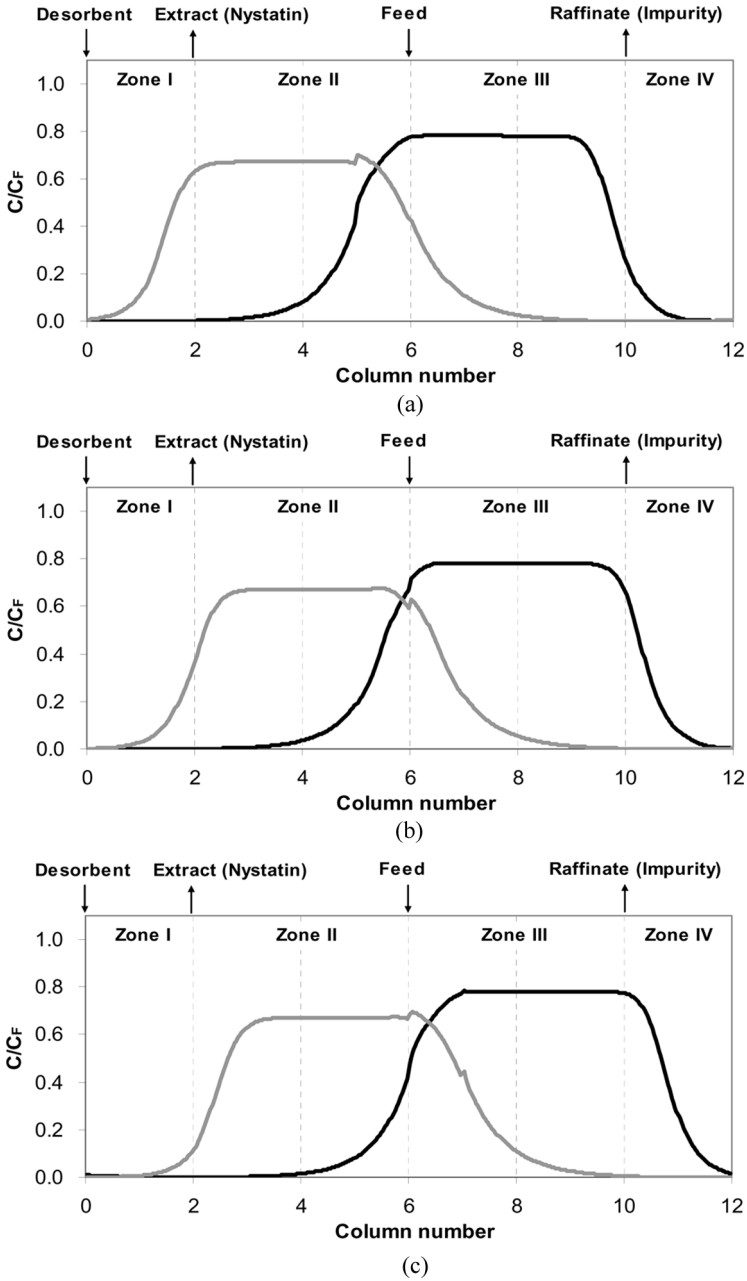

Figure 12. Column profiles of nystatin and impurity at cyclic steady state in the SMB corresponding to the best Pareto solution (dp = 55 μm) under the feed flow rate of 60 mL/min. (a) At the beginning of a step. (b) In the middle of a step. (c) At the end of a step. ——: Nystatin, ——: Impurity.

through the SMB $\leq$ 100 psi. Such a multi-objective optimization task was performed by a highly efficient adaptation of genetic algorithm, NSGA-II-JG.

Since multiple objectives were taken into consideration, the optimization work produced a group of various optimal solutions, i.e., the so called Pareto set. These multiple solutions showed a tradeoff between the two objectives, i.e., the purity and yield of nystatin. The reason for such a phenomenon is that a favorable direction of solute migration (relative to the ports) for higher nystatin purity is opposite to that for higher nystatin yield in the key separation zones, which can be well explicated using the flow rate ratios from the equilibrium theory.

The optimization results were affected largely by the adsorbent particle size. In the region of small particles, the nystatin purities and yields of the SMBs corresponding to the Pareto solutions increase with increasing the particle size. Such a trend occurs because the two objectives are limited by the pressure drop constraint in the region of small particles. By contrast, in the region of large particles, the nystatin purities and yields of the SMBs corresponding to the Pareto solutions decrease with increasing the particle size. This is mostly due to the fact that the two objectives are limited by the mass transfer efficiency (or column efficiency) in the region of large particles, which can be confirmed by the DI values from the SWD equations. As a result, the best Pareto set, which is defined here as the Pareto set surpassing all the other ones in both the nystatin purity and yield, occurs when the particle size falls on the boundary between the pressure limiting and the mass transfer limiting regions.

The effect of throughput (or feed flow rate) on the optimization results was also investigated. As a target throughput is set lower, the nystatin purity and yield are improved and the distribution region of the two objective values on the corresponding best Pareto curve is reduced. As a consequence, the highest purity and yield of nystatin (99.9% each) are attained when the best Pareto curve is converged to only a single point as a result of a significant decrease in the throughput.

NOMENCLATURE

a_{i}	isotherm parameter of component *i* (per solid volume), L/L S.V.
C_F	feed concentration, g/L
d_c	column diameter, cm
d_p	diameter of adsorbent particle, μm
DI	deviation from ideality
D_p	effective pore diffusivity, cm^2/min
E_{b}	axial dispersion coefficient, cm^2/min

k_f	film mass-transfer coefficient, cm/min
K_f	lumped mass-transfer coefficient, min^{-1}
L_c	single column length, cm
m^j	flow rate ratio in zone j
N_c^j	number of columns in zone j
$N_{c,total}$	total number of columns used in SMB unit
NTP	number of theoretical plates
P	phase ratio
Pe	Peclet number
Pur_A	purity of a product component, %
Q_{Feed}	feed flow rate, mL/min
Q^j	volumetric flow rate in zone j, mL/min
R	radius of adsorbent particle, μm
S	cross-sectional area of a column, cm^2
St	Stanton number
t_s	switching time, min
u_0^j	interstitial linear velocity in zone j, cm/min
$u_{w,i}^j$	wave migration velocity of a solute i in zone j, cm/min
$Yield_A$	yield of a product component, %
$Yield_B$	yield of an impurity component, %
ν	port velocity, cm/min
ε_b	inter-particle void fraction
ε_p	intra-particle void fraction
β_i^j	decay factor of component i in zone j
ΔP	total pressure drop through an SMB unit, psi
χ	column configuration

ACKNOWLEDGMENTS

This work was supported by the Korea Research Foundation Grant funded by the Korean Government (MOEHRD, Basic Research Promotion Fund) (KRF-2006–311- D00387). The author is grateful to Prof. Nien-Hwa Linda Wang from Purdue University.

REFERENCES

1. Jensen, T.B.; Reijns, T.G.P.; Billiet, H.A.H.; van der Wielen, L.A.M. Novel simulated moving-bed for reduced solvent consumption. J. Chromatogr. A. **2000**, *873*, 149–162.
2. Michel, G.W. In *Analytical Profiles of Drug Substances*; Florey, K., Ed.; Academic Press: New York, 1977, 341.

3. Mazzotti, M.; Storti, G.; Morbidelli, M. Optimal operation of simulated moving bed units for nonlinear chromatographic separations. J. Chromatogr. A. **1997**, *769*, 3–24.
4. Pais, L.S.; Loureiro, J.M.; Rodrigues, A.E. Modeling strategies for enantiomers separation by SMB chromatography. AIChE J. **1998**, *44*, 561–569.
5. Ruthven, D.M.; Ching, C.B. Counter-current and simulated counter-current adsorption separation processes. Chem. Eng. Sci. **1989**, *44*, 1011–1038.
6. Juza, M.; Mazzotti, M.; Morbidelli, M. Simulated moving bed chromatography and its application to chirotechnology. Trends Biotechnol. **2000**, *18*, 108–118.
7. Goldberg, D.E. *Genetic algorithms in search, optimization, and machine learning*; Addison-Wesley Longman, Inc.: Reading, MA, 1989.
8. Zhang, Z.; Hidajat, K.; Ray, A.K.; Morbidelli, M. Multiobjective optimization of SMB and varicol process for chiral separation. AIChE J. **2002**, *48*, 2800–2816.
9. Kasat, R.B.; Gupta, S.K. Multi-objective optimization of an industrial fluidized-bed catalytic cracking unit (FCCU) using genetic algorithm (GA) with the jumping genes operator. Comput. Chem. Eng. **2003**, *27*, 1785–1800.
10. Zhang, Z.; Mazzotti, M.; Morbidelli, M. Multiobjective optimization of simulated moving bed and varicol processes using a genetic algorithm. J. Chromatogr. A **2003**, *989*, 95–108.
11. Ma, Z.; Wang, N.H.L. Standing wave analysis of SMB chromatography: Linear systems. AIChE J. **1997**, *43*, 2488–2508.
12. Wu, D.J.; Xie, Y.; Ma, Z.; Wang, N.H.L. Design of simulated moving bed chromatography for amino acid separations. Ind. Eng. Chem. Res. **1998**, *37*, 4023–4035.
13. Wankat, P.C. *Rate-controlled separations*; Blackie Academic & Professional: Glasgow, UK, 1990.
14. Hritzko, B.J.; Xie, Y.; Wooley, R.; Wang, N.H.L. Standing wave design of tandem SMB for linear multicomponent systems. AIChE J. **2002**, *48*, 2769–2787.
15. Ergun, S. Flow through packed columns. Chem. Eng. Prog. **1952**, *48*, 89–94.
16. Xie, Y.; Farrenburg, C.A.; Chin, C.Y.; Mun, S.; Wang, N.H.L. Design of SMB for a nonlinear amino acid system with mass transfer effects. AIChE J. **2003**, *49*, 2850–2863.
17. Zhang, Y.; Hidajat, K.; Ray, A.K. Determination of competitive adsorption isotherm parameters of pindolol enantiomers on α_1-aicd glycoprotein chiral stationary phase. J. Chromatogr. A. **2006**, *1131*, 176–184.
18. Kurup, A.S.; Hidajat, K.; Ray, A.K. Comparative study of modified simulated moving systems at optimal conditions for the separation of ternary mixtures under nonideal conditions. Ind. Eng. Chem. Res. **2006**, *45*, 3902–3915.
19. Storti, G.; Masi, M.; Carra, S.; Morbidelli, M. Optimal design of multicomponent countercurrent adsorption separation processes involving nonlinear equilibria. Chem. Eng. Sci. **1989**, *44*, 1329–1345.
20. Mun, S.; Wang, N.H.L.; Koo, Y.M.; Yi, S.C. Pinched wave design of a four-zone SMB for linear adsorption systems with significant mass-transfer effects. Ind. Eng. Chem. Res. **2006**, *45*, 7241–7250.

21. Mun, S. Effect of subdividing the adsorbent bed in a five-zone simulated moving bed chromatography for ternary separation. J. Liq. Chromatogr. & Rel. Technol. **2008**, *31*, 1231–1257.
22. Wilson, E.J.; Geankoplis, C.J. Liquid mass transfer at very low Reynolds numbers in packed beds. Ind. Eng. Chem. Fundam. **1966**, *5*, 9–14.
23. Chung, S.F.; Wen, C.Y. Longitudinal dispersion of liquid flowing through fixed and fluidized beds. AIChE J. **1968**, *14*, 857–866.

Received May 4, 2008
Accepted June 30, 2008
Manuscript 6343